Photoactivatable and Photoconvertible Fluorescent Probes for Protein Labeling

ARTICLE *in* ACS CHEMICAL BIOLOGY · MARCH 2010

Impact Factor: 5.33 · DOI: 10.1021/cb1000229 · Source: PubMed

4 AUTHORS, INCLUDING:

Damien Maurel
Institut de Génomique Fonctionnelle,
34 PUBLICATIONS **1,453** CITATIONS
SEE PROFILE

Sambashiva Banala
Janelia Farm Research Campus
13 PUBLICATIONS **160** CITATIONS
SEE PROFILE

ARTICLE

ACS chemical biology

Photoactivatable and Photoconvertible Fluorescent Probes for Protein Labeling

Damien Maurel[†,§], Sambashiva Banala[†,§], Thierry Laroche[‡], and Kai Johnsson[†,*]

[†]Institute of Chemical Sciences and Engineering, École Polytechnique Fédérale de Lausanne (EPFL), Lausanne, Switzerland and [‡]BioImaging and Optics Platform, EPFL, Lausanne, Switzerland, [§]These authors contributed equally to this work.

ABSTRACT Photosensitive probes are powerful tools to study cellular processes with high temporal and spatial resolution. However, most synthetic fluorophores suited for biomolecular imaging have not been converted yet to appropriate photosensitive analogues. Here we describe a generally applicable strategy for the generation of photoactivatable and photoconvertible fluorescent probes that can be selectively coupled to SNAP-tag fusion proteins in living cells. Photoactivatable versions of fluorescein and Cy3 as well as a photoconvertible Cy5-Cy3 probe were prepared and coupled to selected proteins on the cell surface, in the cytosol, and in the nucleus of cells. In proof-of-principle experiments, the photoactivatable Cy3 probe was used to characterize the mobility of a lipid-anchored cell surface protein and of a G protein coupled receptor (GPCR). This work establishes a generally applicable strategy for the generation of a large variety of different photosensitive fluorophores with tailor-made properties for biomolecular imaging.

Photosensitive fluorescent proteins (FPs) have become important tools in biological research as they permit highlighting of subpopulations of a given protein with optical methods in living cells (*1*). There are three types of photosensitive FPs: photoactivatable, photoconvertible, and photoswitchable FPs. Photoactivatable FPs are those that are transferred from a dark to a bright state with light. Examples are photoactivatable GFP (PA-GFP) and the recently introduced photoactivatable mCherry (PA-mCherry1) (*2, 3*). In contrast, photoconvertible proteins such as Kaede, EosFP, and Dendra change their emission wavelength upon photostimulation, whereas the photoswitchable Dronpa can reversibly be turned on and off with specific illumination (*4–7*). Examples for the use of these three classes of optical highlighters are the measurement of protein diffusion across the nuclear envelope (*2*), the characterization of the recycling of GPCRs (*8*) and the shuttling of G proteins (*9*), the visualization of the trafficking of transporters (*10*), and their application for super-resolution techniques such as PALM (photoactivated localization microscopy) (*1, 3*). Despite their success in biological research, photosensitive FPs have certain limitations. Compared to regular FPs, the existing color palette is limited and among the photoactivatable FPs only PA-GFP and PA-mCherry1 are spectroscopically distinguishable (*3*). Furthermore, most photoconvertible proteins such as Kaede or EosFP show a dual shift of both excitation and emission wavelengths, which makes their application in measurements of fast kinetic processes difficult. This problem has recently been addressed by the introduction of photoconvertible Phamret, which is a fusion protein of cyan FP (CFP) and PA-GFP (*11*). As the pre- and postphotoconverted forms of Phamret have the same excitation wavelengths, it is ideally suited for studying fast dynamic processes. However, drawbacks are its

*Corresponding author, kai.johnsson@epfl.ch.

Received for review January 27, 2010 and accepted March 10, 2010.

Published online March 10, 2010

10.1021/cb1000229

size of 53 kDa and the relatively modest change in the ratio of the fluorescence intensities at the two emission wavelengths (about 12-fold). The size and oligomeric state is also an issue for some of the other photoconvertible proteins, such as tetrameric Kaede, as FP-induced oligomerization can affect the function or localization of the fusion protein (*12*). Finally, the investigation of different properties of a given protein will often require the use of different highlighter proteins, thereby requiring the generation and characterization of multiple fusion proteins for each protein of interest. It would be desirable if a single photosensitive FP would be ideally suited for most, if not all, potential applications.

An alternative approach to generate photosensitive proteins is the specific labeling of proteins with photosensitive synthetic fluorophores. Different methods that permit a specific labeling of fusion proteins with synthetic probes in living cells exist (*13*) and various synthetic fluorophores that are either photoactivatable or photoconvertible have been described in the past (*14–18*). A first example of how this approach can be used for the generation of photosensitive proteins was the labeling of SNAP-tag fusion proteins with photoconvertible nitro-benzospiropyran (nitro-BIPS) derivatives by the group of Marriott (*19*). SNAP-tag is a 20 kDa protein that can be specifically labeled with O^6-benzlyguanine (BG) derivatives, and a BG derivative of nitro-BIPS permitted the attachment of the photoconvertible probe to a fusion protein of SNAP-tag with GFP in living cells. However, to exploit the enormous potential of a combination of protein labeling technologies with synthetic photosensitive fluorophores, additional photosensitive fluorophores that can be derivatized with substrates for protein labeling are needed. Up to now, most photosensitive fluorophores are photoactivatable fluorophores that are fixed in a nonfluorescent configuration through the derivatization with a photocleavable group (*i.e.*, caging). Caged versions of coumarin, fluorescein, and rhodamine have been previously reported (*14, 15, 18*). However, this strategy is not readily applicable for a number of fluorophores that are well-suited for biomolecular imaging such as the cyanine dyes or the Alexa fluorophores, for which no caged versions have been described so far. Furthermore, caging of fluorescein and rhodamine requires the attachment of two photocleavable groups, which complicates the uncaging process. An alternative strategy to generate photoactivatable fluorophores that addresses the aforementioned shortcomings is to connect a fluorophore and a quencher through a photocleavable linker (*20*). Fluorophores and quenchers are chosen such that the emission spectrum of the donor overlaps with the absorption spectrum of the acceptor (quencher). This condition is required to ensure an efficient intramolecular quenching of the fluorophore by dynamic quenching mechanisms (*21*). Here we apply this strategy for the generation of photoactivatable and photoconvertible fluorophores that can be specifically attached to SNAP-tag fusion proteins (Figure 1, panel a). The photosensitivity of the probes is based on photocleavage of a linker between a quencher or a second fluorophore and the fluorophore of interest. The molecules furthermore contain a BG moiety for attachment to SNAP-tag fusion proteins. Following this design principle, photoactivatable versions of fluorescein and Cy3 (Q-Fl and Q-Cy3) and a photoconvertible Cy5-Cy3 probe are introduced. The fluorescence properties of the molecules were characterized *in vitro* and in living cells, and their applicability was tested by measurement of the lateral mobility of the cell surface fusion proteins SNAP-glycosylphosphatidylinositol anchored protein (SNAP-GPI) and SNAP-neurokinin-1 (SNAP-NK1) receptor. This work establishes a generally applicable strategy for the generation of energy transfer-based photoactivatable and photoconvertible organic probes that can be specifically attached to SNAP-tag fusion proteins in living cells and whose emission wavelengths can be readily tailored by choosing appropriate fluorophores.

RESULTS AND DISCUSSION

Design and Synthesis of the Probes. Following the general strategy outlined in Figure 1, panel a, we developed two photoactivatable probes (Q-Fl and Q-Cy3) and one photoconvertible probe (Cy5-Cy3). For the photoactivatable probes we chose QSY7 as nonfluorescent acceptor because this quencher has a broad absorption from 500 to 600 nm and was previously reported to be a good quencher of BODIPY-TMR (see Supplementary Figure 1 for adsorption spectra) (*22*). For the photoconvertible probe, Cy3 and Cy5 fluorophores were selected because these dyes have already been used with success for Förster resonance energy transfer (FRET) microscopy (*23*) and currently no photoconvertible FP exists with such red-shifted emission and excitation wavelengths. For the photocleavable linker we focused on 4,5-dimethoxy-2-nitrobenzyl derivatives (DMNB) as they

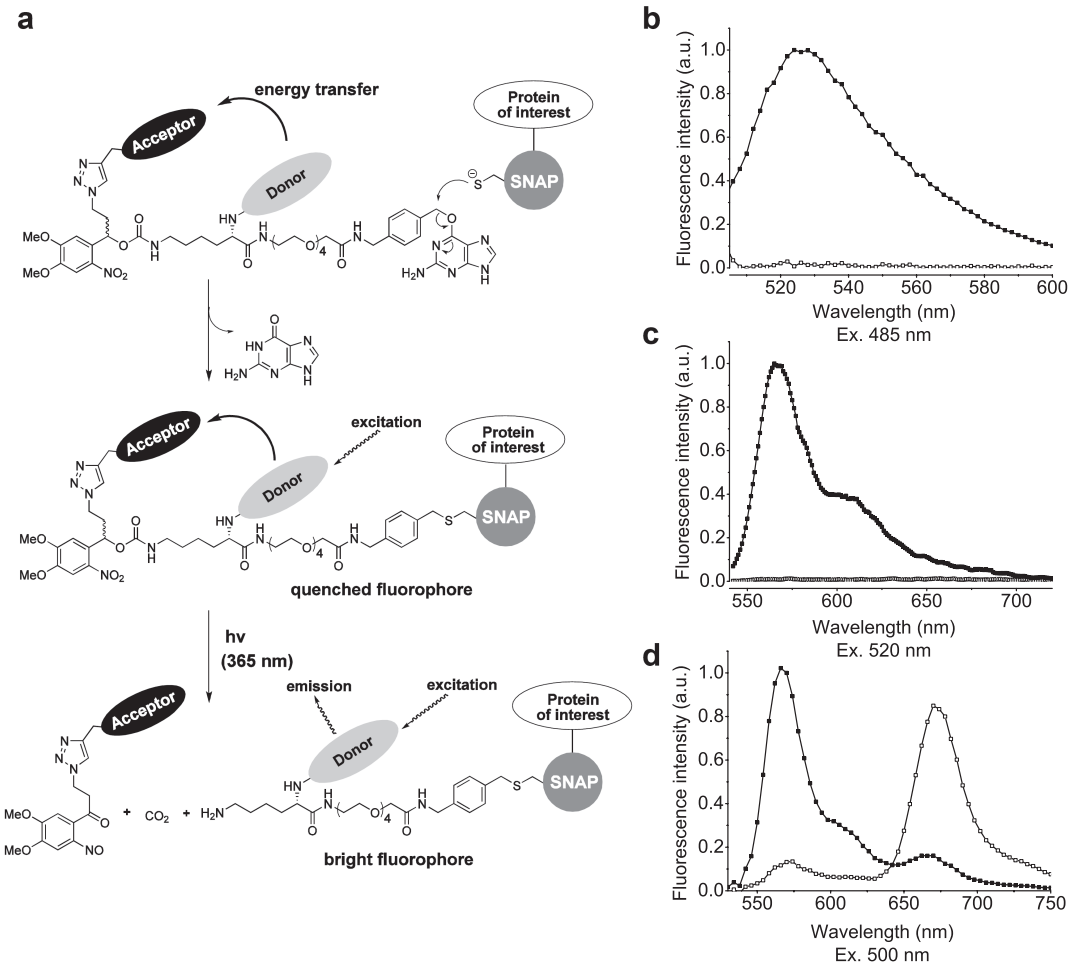

Figure 1. Design of photosensitive fluorophores for SNAP-tag labeling. a) Photoactivatable and photoconvertible probes principle. b–d) Emission spectra of Q-Fl (b), Q-Cy3 (c), and Cy5-Cy3 (d) before (empty symbols) and after (filled symbols) photoactivation (b, c) or photoconversion (d).

possess a high absorption coefficient in the UV region, can be cleaved at wavelengths between 360 and 400 nm (*24*), and show a very fast release of the caged molecule upon irradiation, typically within microseconds (*24–26*). The DMNB group has previously been successfully used in cellular applications (*25, 26*).

The synthesis of our probes is summarized in Figure 2. Starting from commercially available 4,5-dimethoxy-2-nitrobenzaldehyde **4**, intermediate **9** was obtained as a mixture of diastereomers in 5 steps. Compound **9** is an important intermediate as it contains three different functional groups for modification: an azide group for click chemistry, a carboxyl group for coupling to a BG derivative, and a protected amino group that can be used to attach the fluorophore of interest. Accordingly, BG-NH_2 was coupled to the carboxyl group of **9**, which provided compound **10.** The donor was then attached to **10** after deprotection of the Fmoc group. For the final step of the synthesis, the attachment of the acceptor was accomplished *via* click chemistry.

The final photosensitive SNAP-tag substrates, photoactivatable fluorescein **1** (hereafter called Q-Fl), photoactivatable Cy3 **2** (hereafter called Q-Cy3), and the photoconvertible Cy5-Cy3 pair **3** (Cy5-Cy3), were then evaluated for applications in biomolecular imaging.

***In Vitro* Characterization of the Probes and Their SNAP-Tag Conjugates.** The fluorescence properties of the probes before and after coupling to SNAP-tag were

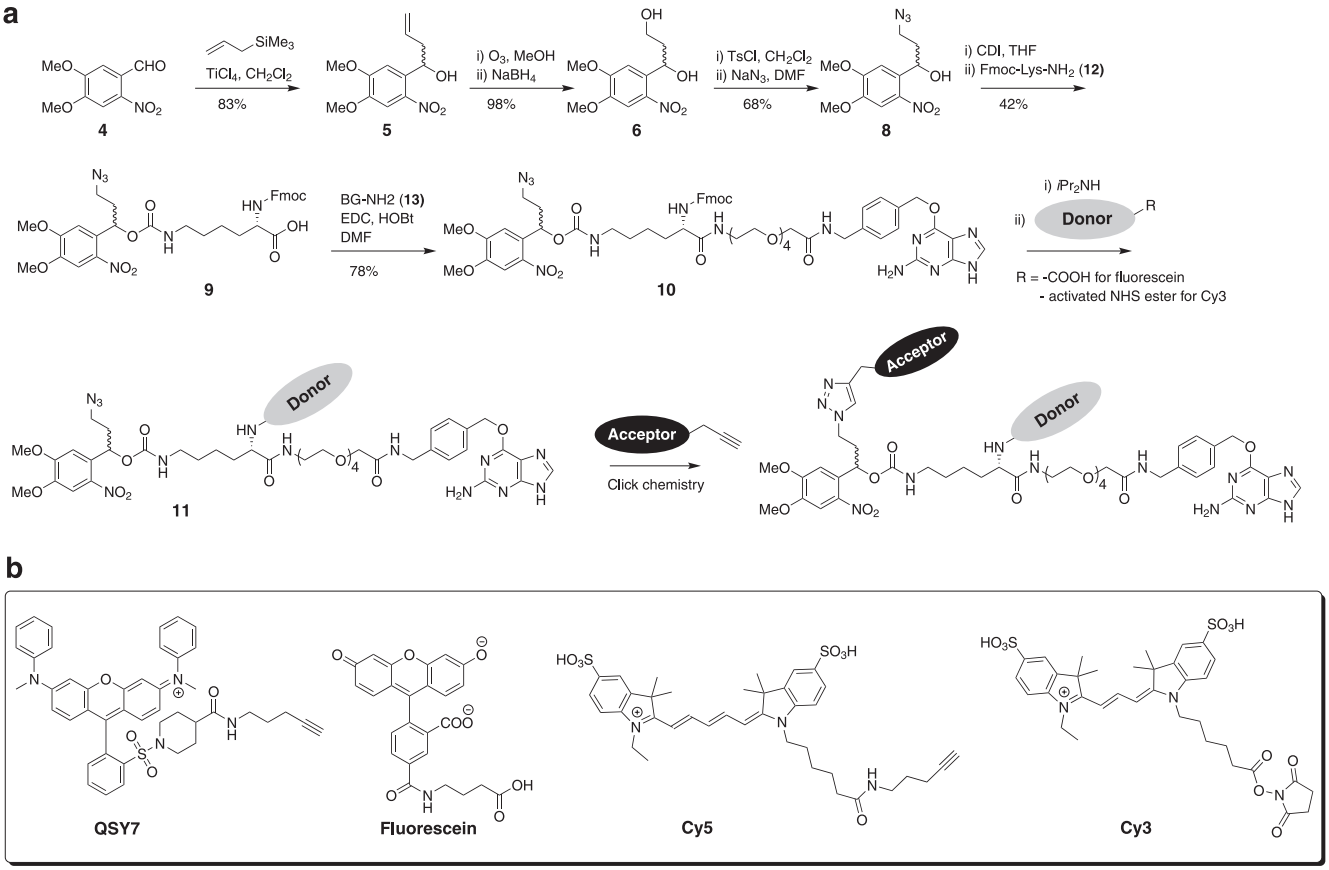

Figure 2. a) Synthesis of photoactivatable and photoconvertable probes. b) Structures of acceptor and donor dyes used in the synthesis. TsCl = *p*-toluenesulphonyl chloride, CDI = 1,1′-carbonyldiimidazole, EDC = *N*-ethyl-*N*′-(3-dimethylaminopropyl)carbodiimide, HOBt =1-hydroxybenzotriazole, *i*Pr$_2$NH = diisopropylamine, DMF = *N*,*N*-dimethylformamide, THF = tetrahydrofuran.

investigated *in vitro* first. The fluorescence intensity of the three probes with BG was measured before and after cleavage of the linker with 365 nm light. Prior to photocleavage, a very weak fluorescence signal was measured from the nonphotoactivated probes, whereupon the illumination produced a large fluorescence increase of the energy donor (Fl, Cy3) and a large decrease of Cy5 emission for the photoconvertible probe (Figure 1, panels b−d). Linker cleavage resulted in a 60-fold and 70-fold increase in fluorescence intensity for Q-Fl and Q-Cy3, respectively (Figure 1, panels b and c). For Cy5-Cy3, the increase of Cy3 and decrease of Cy5 emissions upon irradiation resulted in a 60-fold increase of the Cy3/Cy5 ratio (Figure 1, panel d).

The reactivity of all three derivatives toward SNAP-tag was then tested. We found that these substrates reacted readily with SNAP-tag, although at a rate lower than that of simple BG derivatives (Supplementary Figures 2 and 3). The second-order rate constants for the reaction of SNAP-tag with Q-Fl and Q-Cy3 were measured to be $k = 600\ M^{-1}\ s^{-1}$, with Cy5-Cy3 $k = 4{,}500\ M^{-1}\ s^{-1}$, and for the reaction with a simple BG-Cy3 derivatives $k = 4{,}500\ M^{-1}\ s^{-1}$ (Supplementary Figure 3).

To study the properties of the probes after reaction with SNAP-tag, an excess of SNAP-tag was incubated with the photosensitive probes and subsequently irradiated with 365 nm light, and the emission spectra were recorded. The fluorescence increase for the SNAP-tag bound photoactivatable probes Q-Fl and Q-Cy3 upon photocleavage of the linker was higher than for the free substrates: 90-fold for Q-Fl and 100-fold for Q-Cy3 (Supplementary Figure 4). The increase of the ratio of the Cy3 and Cy5 emissions measured for photoconvertible SNAP-tag-bound Cy5-Cy3 was 30-fold. The slightly larger increase in fluorescence intensity for the SNAP-tag bound photoactivatable probes might be due to the elimination of the guanine from the photosensitive probe in the course of the protein labeling. It has previ-

ously been observed that guanine can quench fluorophores (*27–29*).

Photoactivation and Photoconversion of SNAP-Tag Bound Probes in Living Cells. The permeability of fluorophores used for protein labeling is a key property for cellular applications. For example, impermeant dyes are preferable for investigating cell surface proteins as they enable discrimination between cell surface proteins properly folded and those retained in the intracellular compartments or already internalized. This has been exploited, for example, for the analysis of the oligomeric assembly of GPCRs (*30*). In contrast, permeant dyes permit facile labeling also of intracellular proteins. We chose CHO-K1 cells to determine the permeability of our substrates. For that purpose CHO-K1 cells were transfected with a plasmid encoding for a SNAP-FRB fusion protein that is localized in the nucleus and cytosol of the cell. We found that all three probes are impermeable; only insignificant amounts of intracellular SNAP-FRB proteins were labeled after the incubation of the cells with Q-Fl, Q-Cy3 and Cy5-Cy3 (Supplementary Figure 5). However, a strong intracellular labeling with these substrates was detected after permeabilization of the cell's plasma membrane by fixation with formaldehyde. These results are in agreement with previous data obtained with Cy3 and Cy5 BG derivatives (*31*), confirming the inability of these polar dyes to cross cell membranes.

In contrast to the results with intracellular proteins, an efficient and specific cell surface labeling of SNAP-GPI anchored protein can be observed after incubation of cells with Q-Fl, Q-Cy3, and Cy5-Cy3 (Figure 3). For each substrate the fluorescence signal at the plasma membrane was quantified after photocleavage (see Methods). A fluorescence increase of around 20 over background was determined for Q-Fl and Q-Cy3, and the Cy3/Cy5 ratio also increased by a factor of 20.

A practical problem of photactivatable probes is the difficulty in identifying labeled cells or labeled subcellular structures as the probes are very weakly fluorescent prior to photoactivation. Chemical labeling allows one to overcome this problem as cells can be co-labeled with a mixture of quenched fluorescent probe and a second fluorescent SNAP-tag substrate with a distinct emission wavelength (Figure 3, panel d). Alternatively, transfected cells can be identified by co-transfection with a second plasmid encoding, for example, a cytoplasmic GFP as a transfection marker (Supplementary Figure 6). However, this only permits identification of the transfected cells,

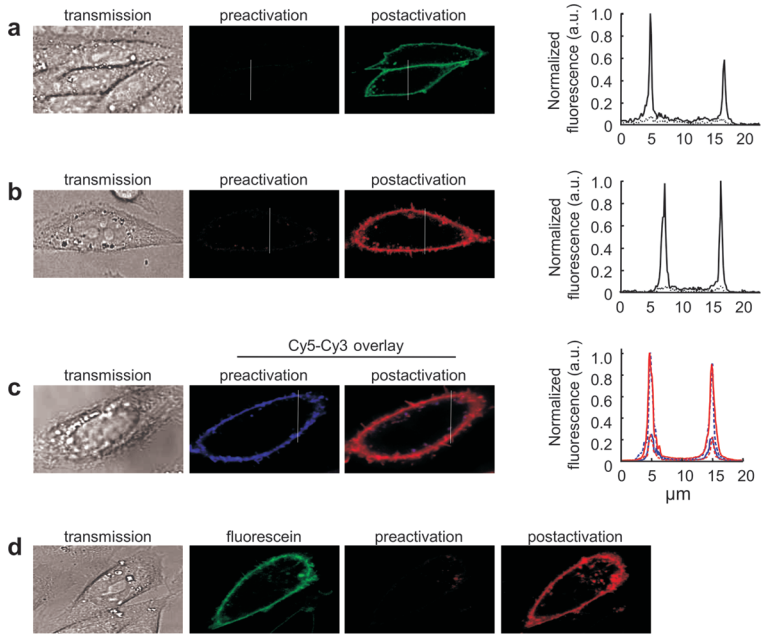

Figure 3. Live cell imaging of cell surface proteins labeled with photosensitive probes. CHO-K1 cells expressing SNAP-GPI were labeled with Q-Fl (a), Q-Cy3 (b), and Cy5-Cy3 (c) and imaged before and after a low intensity pulse of photoactivation. Q-Fl (a), Q-Cy3 (b), and Cy5-Cy3 (c) fluorescence intensities were measured along the white line (1 μm width) on a single cell before and after UV illumination. The dashed and filled lines (right panel) represent the fluorescence intensities before and after photoactivation or photoconversion, respectively. For Cy5-Cy3; overlay of Cy5 (blue) and Cy3 (red) channels is shown. d) Identifying cells expressing SNAP-GPI prior to photoactivation through simultaneous double labeling. CHO-K1 cells transiently transfected with SNAP-GPI were labeled with a mixture of Q-Cy3 (5 μM) and BG-fluorescein (0.1 μM). Labeled CHO-K1 cells were identified through fluorescein detection (green channel) and then briefly illuminated with UV light to activate Cy3 fluorescence.

whereas co-labeling precisely reveals the location of the protein of interest.

Unlike photoactivatable probes, the photoconvertible Cy5-Cy3 probe can be tracked and imaged *via* its Cy5 emission prior to photoconversion. A conceptual difference between our photoconvertible probe and photoconvertible FPs is the release of Cy5 upon photocleavage. In the case of Cy5-Cy3 labeled SNAP-GPI, photoconversion of probe bound to cell surface proteins results in rapid diffusion of released Cy5 away from the cell. However, once the Cy5-Cy3 protein is internalized and subsequently photoconverted, released Cy5 remains trapped inside vesicles (Supplementary Figure 7). This is an attractive feature as, for example, the released Cy5 should permit following the fate of the

soluble content of lumenal vesicles, whereas the Cy3 reports on the membrane-bound protein of the vesicle.

The value of the photosensitive probes introduced here would be significantly increased if they could be used for the labeling of intracellular proteins. Different cell-loading techniques have been reported to introduce impermeant molecules into living cells (*32, 33*). Previously, nuclear SNAP-tag fusion proteins were labeled with impermeant fluorophores through microinjection of the dyes (*31*). Here we decided to focus on a technique called bead-loading, which has already been used to load fluorophores into mammalian cells (*34*). This approach is attractive as it requires no special equipment and is very simple to implement. Bead-loading relies on temporary membrane disruptions by mechanical friction with glass beads, thereby creating a direct access to a cell's cytoplasm. We speculated that during a subsequent recovery period any excess of BG derivatives would also be pumped out of cells as has been observed after microinjection (*31*). This point is essential for the success of this approach as the presence of an excess of free fluorophores inside the cells would mask the specific localization of the proteins of interest.

To demonstrate the ability to label SNAP-tag fusion proteins with our photosensitive probes inside living cells, CHO-K1 cells were co-transfected with either SNAP-NLS or SNAP-MEK1, proteins that are localized in the nucleus or cytoplasm, respectively (*35*), and the cell surface protein CLIP-GPI as a transfection marker. CLIP-tag is an alternative self-labeling protein that can be specifically labeled in the presence of SNAP-tag with a different class of substrates, O^2-benzylcytosine (BC) derivatives (*36*). Transfected cells were subjected to bead-loading of Q-Fl and then incubated for 2 h in culture medium. To identify transfected cells, CLIP-GPI was labeled with BC-Cy3 as Q-Fl is weakly fluorescent before photoactivation. As shown in Figure 4, SNAP-NLS and SNAP-MEK1 fusion proteins can be specifically labeled with Q-Fl in live cells and subsequently photoactivated. The localization of the photoactivated protein indicates the specificity of the labeling. It should be noted that only a fraction (about 15%) of the transfected cells were loaded with Q-Fl. However, loaded cells and labeled SNAP-tag can be easily identified by the addition of a spectroscopically distinguishable and impermeant fluorescent SNAP-tag substrate during bead-loading (Figure 4, panel c). Together, these experiments demonstrate how impermeant Q-Fl can be used for the labeling of cytosolic and nuclear SNAP-tag fusion proteins, which significantly expands the field of application for our photosensitive probes.

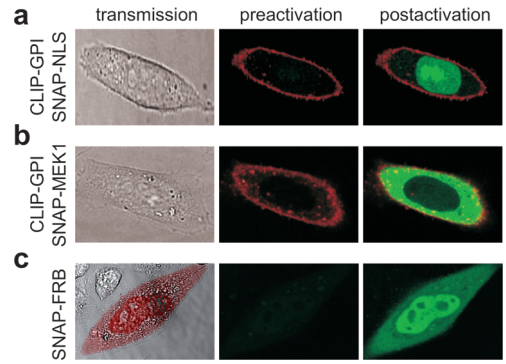

Figure 4. Labeling of cytosolic and nuclear SNAP-tagged proteins with Q-Fl in living cells. CHO-K1 cells co-transfected with CLIP-GPI and SNAP-NLS (a) or with CLIP-GPI and SNAP-MEK1 (b) were loaded with Q-Fl through bead-loading. After bead-loading, cells were incubated at 37 °C in culture medium for 2 h. CLIP-GPI fusion proteins expressed at the cell surface were then labeled with a non-permeable BC-Cy3 substrate to reveal the transfected cells. Left panels represent transmission images; middle and right panels represent the overlay of Q-Fl (green) with Cy3 (red) before and after photoactivation, respectively. c) CHO-K1 cells transfected with SNAP-FRB were loaded with a mixture of Q-Fl (50 μM) and BG-Cy3 (5 μM). Left panel represents the overlay of transmission images with Cy3; middle and right panels represent Q-Fl emission before and after photoactivation, respectively.

As mentioned above, impermeant dyes present several advantages to track proteins specifically at the cell surface (*30*). As a proof-of-principle application we used our molecules to determine the lateral mobility of cell surface proteins such as SNAP-GPI and SNAP-NK1. Fluorescence recovery after photobleaching (FRAP) is commonly used to examine protein dynamics in living cells. However, this approach can be considered as an indirect method to measure the mobility of a protein as the fluorescence recovery within the bleached region arises from molecules located in adjacent regions. In the case of cell surface proteins, fluorescence recovery can result from the lateral movement of proteins but also from the insertion of new proteins into the plasma membrane. Photoactivation of chemically labeled cell surface proteins permits to overcome this problem as only photoactivated molecules originating from the highlighted region at the cell surface can be tracked.

To examine whether Q-Cy3 and Cy5-Cy3 substrates are suitable to track cell surface proteins, we determined the time course of the fluorescence increase after photocleavage (Supplementary Figure 8). A brief UV illumination (200 ms) of a whole cell using a 405 nm diode laser generated an instant and readily detectable increase in fluorescence intensity. With illumination at 543 nm, the signal remained constant over time, illustrating that Cy3 is a very photostable dye. Furthermore, repeated illuminations at 405 nm demonstrated that only a fraction of the photosensitive dyes was activated under these conditions. Nevertheless, the possibility to photoactivate our probes with a 405 nm diode laser is advantageous as most confocal microscopes are equipped with such a laser.

We then used Q-Cy3 to examine the diffusion of SNAP-GPI and SNAP-NK1 at the cell surface. These two fusion proteins are interesting models as lipid-anchored proteins diffuse more rapidly than transmembrane proteins (*37*). After labeling with Q-Cy3, the two SNAP-tagged proteins were illuminated with a brief photoactivation pulse at 405 nm light (1 s) delivered to a small spot (3 μm diameter) at the basal membrane (Figure 5). The change in fluorescence intensity was monitored over time in this small region of interest (ROI), and the diffusion coefficient was calculated (Table 1 and Methods). The diffusion of SNAP-GPI, with a diffusion coefficient of 0.250 $\mu m^2\ s^{-1}$ ± 0.099, is significantly faster than that measured for SNAP-NK1, which has a diffusion coefficient of 0.046 $\mu m^2\ s^{-1}$ ± 0.014. We independently determined a similar mobility for these two fusion proteins using FRAP microscopy (Figure 5). For these experiments, proteins were labeled with BG-Cy3, and the bleaching was performed with a 488 nm laser line. The different diffusion coefficients measured in these experiments are summarized in Table 1. The results are in agreement with previously reported data for proteins that belong to the same family (*38, 39*). Furthermore, we also measured the diffusion coefficient of SNAP-NK1 using the photoconvertible Cy5-Cy3. Here, the mobility of NK1 receptors was determined by applying a photoconversion pulse at 405 nm light (1 s) delivered to a small spot

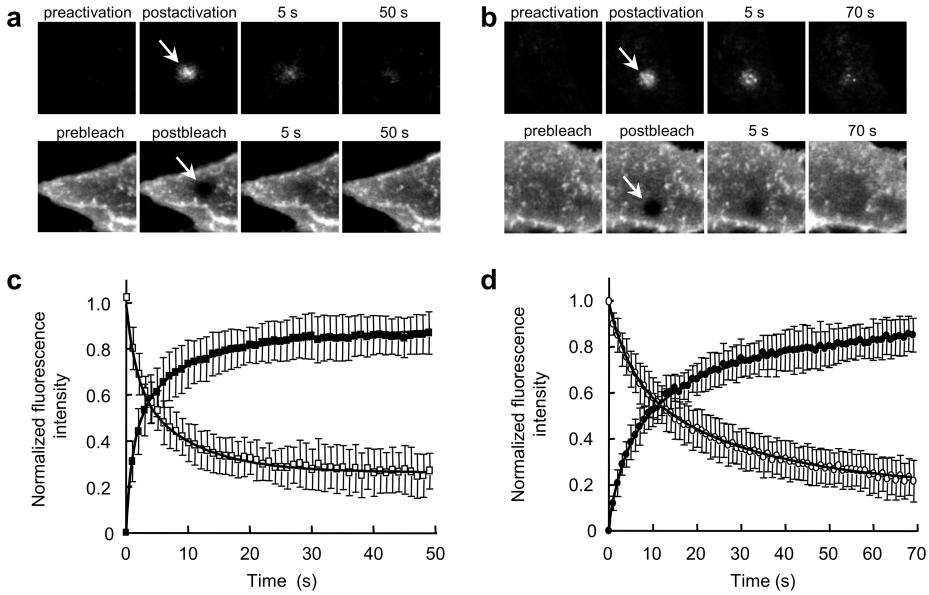

Figure 5. Measuring the diffusion of plasma membrane proteins by photoactivation or photobleaching. CHO-K1 cells expressing SNAP-GPI or SNAP-NK1 were labeled with Q-Cy3 and BG-Cy3 for photoactivation and photobleaching experiments, respectively. (a) Representative photoactivation (top) and FRAP (bottom) experiments for SNAP-GPI (a) and SNAP-NK1 (b). A 3 μm circle was photoactivated at 405 nm or bleached at 488 nm, and the fluorescence was monitored for the indicated time periods. Arrows indicate the region of photoactivation and bleaching. Fluorescence images of cells were acquired at 37 °C on an inverted confocal microscope (Zeiss, LSM510). Fluorescence decay and recovery curves were determined for SNAP-GPI (c) and SNAP-NK1 (d). The ratio between mean fluorescence intensity of the photoactivated and bleached circles and the mean fluorescence of the whole cell were normalized to the preactivation and prebleach ratio, respectively. The curves are nonlinear regression fits to the normalized data (see Methods). The curves represent the means ± SD of at least 15 independent cells for each protein.

TABLE 1. Lateral mobility of plasma membrane proteins

Construct	Dye	Method	D ($\mu m^2\ s^{-1}$)[a,c]	MF (%)[b,c]
SNAP-GPI	Q-Cy3	Photoactivation	0.250 ± 0.099	77 ± 13
	Cy3	Photobleaching	0.240 ± 0.109	92 ± 07
SNAP-NK1	Q-Cy3	Photoactivation	0.046 ± 0.014	81 ± 09
	Cy3	Photobleaching	0.052 ± 0.014	89 ± 12
SNAP-NK1	Cy5-Cy3	Photoconversion (Cy5)	0.055 ± 0.014	94 ± 07
		Photoconversion (Cy3)	0.051 ± 0.013	96 ± 04

[a]Diffusion coefficient expressed as mean ± SD. [b]Mobile fraction (mean ± SD). [c]Mean values and SD were calculated from diffusion values obtained independently on at least 15 cells.

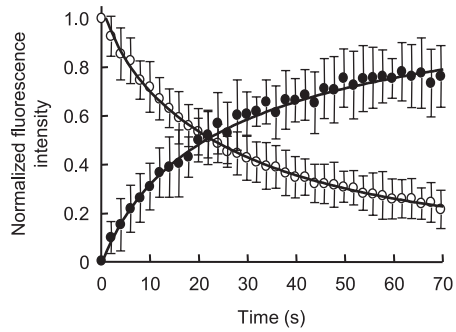

Figure 6. SNAP-NK1 diffusion measured with Cy5-Cy3. CHO-K1 expressing SNAP-NK1 were labeled with Cy5-Cy3. A 4 μm circle was photoactivated at 405 nm, and the fluorescence was monitored simultaneously in Cy5 (filled circles) and Cy3 (open circles) channels. The curves are nonlinear regression fits to the normalized data (see Methods). The curves represent the means ± SD of 18 independent cells.

(4 μm diameter) at the basal membrane and subsequent recording of Cy3 and Cy5 fluorescence with a continuous Cy3 illumination (Figure 6). These experiments demonstrate how the photoactivatable and photoconvertible probes introduced here can be used for measuring protein mobility and dynamic processes in living cells.

In summary, we have established a straightforward synthesis for the generation of a large palette of photoactivatable and photoconvertible probes suitable for protein labeling in living cells. These probes offer spectroscopic properties that cannot be found in currently available photoconvertible FPs, an example being the photoconvertible Cy5-Cy3. We have demonstrated the use of these probes for the labeling of SNAP-tag fusion proteins on cell surfaces as well as inside living cells. Furthermore, we showed the application of the resulting photoactivatable and photoconvertible SNAP-tag fusion proteins to measure protein mobility on the cell surface. Importantly, our photosensitive probes, together with previously introduced SNAP-tag substrates, enable the use of the same SNAP-tag construct for a large variety of different experiments utilizing photoactivation, photoconversion, photobleaching, pulse-chase labeling, or FRET. The here introduced probes thus significantly broaden the possibilities offered through chemical labeling to study protein function in living cells.

METHODS

Synthesis. Detailed synthetic procedures and characterizations are described in Supporting Information.

***In Vitro* Fluorescence Measurements.** Fluorescence spectra were measured on a SpectraMax (Molecular Device) fluorescence reader. Solutions of the probes (final concentration of 1 μM) were diluted in 50 mM HEPES buffer (pH 7.4) with 50 mM NaCl, 1 mM dithiothreitol (DTT), and 0.2 mg mL^{-1} bovine serum albumin (BSA) and irradiated at different time durations with 365 nm light from a HBO 100-W Hg lamp. To selectively obtain 365 nm light from the Hg lamp, 345 nm long pass filter and 400, 500, and 600 nm short pass filters were used. Fluorescence intensities were measured in 96-well plates (Becton Dickson) containing 100 μL of solution in each well. The increase of the fluorescence upon irradiation was determined from the integrated fluorescence intensity, from 510−550 nm for Q-Fl, and 550−580 nm for Q-Cy3. Fluorescence ratio change was determined using the following formula: $(R_{\text{fluorescence}(670/570)})_{\text{before UV}}/(R_{\text{fluorescence}(670/570)})_{\text{after UV}}$. For recording the fluorescence after reaction with SNAP-tag, we expressed and purified the GST-SNAP fusion protein as previously described (*40*). The labeling reaction was carried out at RT: 3 μM of SNAP-tag was incubated with 1 μM of substrate at RT for 3 h. Samples were then irradiated with 365 nm light for different time durations and fluorescence was recorded as described above.

***In Vitro* Kinetic Analysis.** Recombinant GST-SNAP (0.2 μM) was incubated with 2 μM Q-Cy3, Q-Fl or Cy5-Cy3 in reaction buffer (50 mM HEPES, 1 mM DTT, 0.2 mg mL^{-1} BSA, pH 7.4) at RT. Aliquots were taken at different times, and the reaction was quenched by addition of 20 μM BG-Cy5 for Q-Fl, 20 μM BG-fluorescein for Q-Cy3, and 20 μM O^6-BG for Cy5-Cy3. Aliquots were then boiled at 95 °C for 5 min in SDS loading buffer and analyzed by SDS-PAGE and fluorescence gel imaging. The reaction progress curves for Q-Fl and Q-Cy3 were determined by the fluorescence decrease overtime of Cy5 and fluorescein, respectively. A pseudo-first-order reaction model was applied to fit the curves. For Cy5-Cy3 the fluorescence intensity of Cy5 was used for the analysis. Second-order rate constants were then obtained by dividing the pseudo-first-order constants by the concentration of Q-Fl, Q-Cy3 and Cy5-Cy3.

Plasmids Used. SNAP-GPI (*40*), SNAP-NLS (*36*), SNAP-FRB (*41*), and SNAP-MEK1 (*41*) plasmids used for mammalian expression have been previously described. SNAP-NK1 plasmid was obtained from Covalys. The plasmid encoding CLIP-GPI was generated from the SNAP-GPI plasmid.

Cell Culture and Transfection. Adherent Chinese Hamster Ovary (CHO)-K1 cells were grown in Ham's F12 medium (Lonza) supplemented with 10% fetal bovine serum (Lonza), 1% penicillin-streptomycin and transfected by using Lipofectamine (Invitrogen) according to manufacturer's protocol.

Confocal Microscopy and Live Cell Imaging. Three different microscopes were used to image cells labeled with photoactivatable (Q-Fl, Q-Cy3) and photoconvertible (Cy5-Cy3) probes. Images were collected on a Leica SP5 WLL confocal microscope equipped with a 63X HCX plan Apochromat oil immersion objective lens for signal quantification while dynamic experiments were performed on a Zeiss LSM510 META equipped with a 63X plan Apochromat 1.4 NA oil immersion objective lens or on a Leica SP2 laser scanning confocal microscope equipped with the same objective as the SP5. Leica SP5 WLL microscope was used with a 488 nm line for excitation of Q-Fl, a 543 nm line for exci-

tation of Q-Cy3, and a 520 nm line for excitation of Cy5-Cy3. Photoactivation of probes was performed with a 120-W Xcite external Halogen lamp with a 340−380 nm excitation band-pass. Fluorescence was collected at 500−560 nm for Q-Fl and 560−660 nm for Q-Cy3. For the photoconvertible Cy5-Cy3 probe fluorescence was recorded at 540−620 nm for Cy3 and 650−750 nm for Cy5. Mobility studies with Q-Cy3 and BG-Cy3 were performed on the LSM510 META using a 1-mW HeNe laser 543 nm (Lasos) for excitation and 25-mW diode laser 405 nm (Lasos) for Q-Cy3 photoactivation, whereas photobleaching of Cy3 was carried out with the 488 nm argon laser line. The emission beam was split with a NFT 545 dichroic mirror and recorded on a detector with a long-pass filter (LP560). Fluorescence signal of Cy5-Cy3 for the mobility studies was done on a SP2 microscope with the following settings: 514 nm argon laser for Cy3 excitation, 405 nm diode laser for photoconversion, and fluorescence recorded at 540−620 nm for Cy3 and 650−750 nm for Cy5.

CHO-K1 cells seeded at a rate of 150,000 cells per μ-Dish (Ibidi) were transfected with SNAP-GPI or SNAP-NK1. After being labeled with 5 μM Q-Cy3 or Q-Fl or 1 μM Cy5-Cy3 in complete Ham's F12 medium for 10 min at 37 °C, cells were washed three times with Hanks Balanced Salt Solution (HBSS, Lonza) complemented with 1% FBS and imaged in this buffer. Photoactivation and photobleaching experiments were performed at 37 °C with the confocal zoom set to 3. To assay the lateral mobility of SNAP-GPI and SNAP-NK1 at the basal membrane of CHO-K1 cells, a circle of 3 μM diameter was photoactivated using 20 scans with the 405 nm laser line or photobleached using 20 iterations with the 488 nm laser line for Q-Cy3 and Cy3, respectively, at full laser power. Pre- and postbleach images were monitored at low laser intensity with a rate of one frame per second during 60 s for SNAP-GPI and 80 s for SNAP-NK1. Fluorescence intensity in the photoactivated and photobleached region, the overall fluorescence of the whole cell, and the background outside the cell were quantified by using the Zeiss LSM software (Carl Zeiss, MicroImaging, Inc.). The half-time of fluorescence recovery and decay were determined on the basis of the following equations (*42*):

$$F(t) = [F(\infty) - F(0)][\exp(-2\tau_d/t)(I_0(2\tau_d/t) + I_1(2\tau_d/t)] + F(0) \quad \text{for photobleaching}$$

$$F(t) = F(\infty) - F(0)][1 - \exp(-2\tau_d/t)(I_0(2\tau_d/t) + I_1(2\tau_d/t)] + F(0) \quad \text{for photoactivation}$$

where $F(t)$ is the background-corrected and normalized fluorescence intensity at time t in the photoactivated and photobleached ROI, $F(\infty)$ is the fluorescence intensity at the asymptote of the fluorescence recovery and decay curves, $F(0)$ is the fluorescence intensity directly after photobleaching and photoactivation in the ROI, and τ_d is the characteristic diffusion time. I_0 and I_1 are modified Bessel functions. Diffusion coefficient (D) was determined from the equation (*42, 43*):

$$D = 0.224r^2/t_{1/2}$$

where r is the radius of the bleached and photoactivated region and $t_{1/2}$ corresponds to the half-fluorescence recovery and decay time.

Fluorescence Quantification at the Plasma Membrane of CHO-K1 using Metamorph 7.6 Software. Quantification of the fluorescence increase of our substrates at the plasma membrane upon photoactivation was achieved with the following settings: a region in the background (outside the cell) and the mean value of this region were evaluated. This value was subtracted from the images obtained before and after photoactivation. The "mask" of the membrane was evaluated on the positive image (after photoactivation): before the image was denoised (low pass filter, 5X5). Then a threshold was applied to roughly define the membrane area. This area was then "cleaned": borders were smoothed through morphological operators and elements in the background above threshold were reduced through morphological erosion and filtered away by size. The membrane "mask" evaluated on the positive image was then applied to the positive and the negative images (before photoactivation) corrected for the background. The sums of intensities in the membrane regions were evaluated and used to calculate the fluorescence increase upon photoactivation by dividing the signal of the positive images (after photoactivation) with the signal of the negative images (before photoactivation).

Cell Membrane Permeability Studies. CHO-K1 expressing SNAP-FRB were washed twice with culture medium and labeled 30 min at 37 °C with 5 μM Q-Cy3 or Q-Fl or 1 μM Cy5-Cy3 before and after cells fixation with 4% paraformaldehyde solution for 20 min at RT. After being labeled, cells were washed twice and incubated in PBS, 1% FBS in the dark for 20 min at RT. Fixation step of the cells was also followed by washes in PBS. Imaging was performed for each sample on an inverted confocal microscope (Leica, SP5) after a short (2 s) UV light illumination (340−380 nm). Signal was directly quantified on the Leica software.

Glass Beads Loading. CHO-K1 cells co-transfected with CLIP-GPI and SNAP-NLS or SNAP-MEK1 were seeded in μ-Dish (Ibidi) like mentioned above. Twenty-four hours after transfection, 100 μL of the loading solution composed of culture medium supplemented with 50 μM Q-Fl substrate was added onto the cells. Immediately after, glass beads (100 μm diameter) were sprinkled onto the cells. After shaking the coverslips 3−4 times so that the beads roll over the cells, beads were removed by washing 4−5 times with prewarmed culture medium and cells were then incubated at 37 °C, 5% CO_2. A minimum of 2 h after bead loading, CLIP-GPI anchored proteins were labeled with BC-Cy3 (5 μM) for 10 min at 37 °C. After 3 washing steps with complete medium to remove the excess of free BC-Cy3, HBSS buffer complemented with 1% FBS was added onto the cells, and images were taken on a inverted confocal microscope (Leica, SP5) as described above. For co-labeling experiments, a SNAP-FRB fusion protein was expressed alone in CHO-K1 cells, and cells were loaded with a mixture of 5 μM BG-Cy3 with 50 μM Q-Fl.

Acknowledgment: The authors would like to thank Dr. M. Kamiya, Dr. A. Gautier, Dr. M. J. Hinner, and Dr. G. Lukinavicius for helpful discussions and technical assistance. This work was supported by the Swiss National Science Foundation and LipidX.

Supporting Information Available: This material is available free of charge *via* the Internet at http://pubs.acs.org.

REFERENCES

1. Shaner, N. C., Patterson, G. H., and Davidson, M. W. (2007) Advances in fluorescent protein technology, *J. Cell Sci. 120*, 4247–4260.
2. Patterson, G. H., and Lippincott-Schwartz, J. (2002) A photoactivatable GFP for selective photolabeling of proteins and cells, *Science 297*, 1873–1877.
3. Subach, F. V., Patterson, G. H., Manley, S., Gillette, J. M., Lippincott-Schwartz, J., and Verkhusha, V. V. (2009) Photoactivatable mCherry for high-resolution two-color fluorescence microscopy, *Nat. Methods 6*, 153–159.

4. Ando, R., Hama, H., Yamamoto-Hino, M., Mizuno, H., and Miyawaki, A. (2002) An optical marker based on the UV-induced green-to-red photoconversion of a fluorescent protein, *Proc. Natl. Acad. Sci. U.S.A. 99*, 12651–12656.
5. Ando, R., Mizuno, H., and Miyawaki, A. (2004) Regulated fast nucleocytoplasmic shuttling observed by reversible protein highlighting, *Science 306*, 1370–1373.
6. Gurskaya, N. G., Verkhusha, V. V., Shcheglov, A. S., Staroverov, D. B., Chepurnykh, T. V., Fradkov, A. F., Lukyanov, S., and Lukyanov, K. A. (2006) Engineering of a monomeric green-to-red photoactivatable fluorescent protein induced by blue light, *Nat. Biotechnol. 24*, 461–465.
7. Wiedenmann, J., Ivanchenko, S., Oswald, F., Schmitt, F., Rocker, C., Salih, A., Spindler, K. D., and Nienhaus, G. U. (2004) EosFP, a fluorescent marker protein with UV-inducible green-to-red fluorescence conversion, *Proc. Natl. Acad. Sci. U.S.A. 101*, 15905–15910.
8. Schmidt, A., Wiesner, B., Weisshart, K., Schulz, K., Furkert, J., Lamprecht, B., Rosenthal, W., and Schulein, R. (2009) Use of Kaede fusions to visualize recycling of G protein-coupled receptors, *Traffic 10*, 2–15.
9. Chisari, M., Saini, D. K., Kalyanaraman, V., and Gautam, N. (2007) Shuttling of G protein subunits between the plasma membrane and intracellular membranes, *J. Biol. Chem. 282*, 24092–24098.
10. Chudakov, D. M., Verkhusha, V. V., Staroverov, D. B., Souslova, E. A., Lukyanov, S., and Lukyanov, K. A. (2004) Photoswitchable cyan fluorescent protein for protein tracking, *Nat. Biotechnol. 22*, 1435–1439.
11. Matsuda, T., Miyawaki, A., and Nagai, T. (2008) Direct measurement of protein dynamics inside cells using a rationally designed photoconvertible protein, *Nat. Methods 5*, 339–345.
12. Mizuno, H., Sawano, A., Eli, P., Hama, H., and Miyawaki, A. (2001) Red fluorescent protein from Discosoma as a fusion tag and a partner for fluorescence resonance energy transfer, *Biochemistry 40*, 2502–2510.
13. O'Hare, H. M., Johnsson, K., and Gautier, A. (2007) Chemical probes shed light on protein function, *Curr. Opin. Struct. Biol. 17*, 488–494.
14. Gee, K. R., Weinberg, E. S., and Kozlowski, D. J. (2001) Caged Q-rhodamine dextran: a new photoactivated fluorescent tracer, *Bioorg. Med. Chem. Lett. 11*, 2181–2183.
15. Kobayashi, T., Urano, Y., Kamiya, M., Ueno, T., Kojima, H., and Nagano, T. (2007) Highly activatable and rapidly releasable caged fluorescein derivatives, *J. Am. Chem. Soc. 129*, 6696–6697.
16. Marriott, G., and Ottl, J. (1998) Synthesis and applications of heterobifunctional photocleavable cross-linking reagents, *Methods Enzymol. 291*, 155–175.
17. Mitchison, T. J., Sawin, K. E., Theriot, J. A., Gee, K., and Mallavarapu, A. (1998) Caged fluorescent probes, *Methods Enzymol. 291*, 63–78.
18. Zhao, Y., Zheng, Q., Dakin, K., Xu, K., Martinez, M. L., and Li, W. H. (2004) New caged coumarin fluorophores with extraordinary uncaging cross sections suitable for biological imaging applications, *J. Am. Chem. Soc. 126*, 4653–4663.
19. Mao, S., Benninger, R. K., Yan, Y., Petchprayoon, C., Jackson, D., Easley, C. J., Piston, D. W., and Marriott, G. (2008) Optical lock-in detection of FRET using synthetic and genetically encoded optical switches, *Biophys. J. 94*, 4515–4524.
20. Pellois, J. P., Hahn, M. E., and Muir, T. W. (2004) Simultaneous triggering of protein activity and fluorescence, *J. Am. Chem. Soc. 126*, 7170–7171.
21. Johansson, M. K., and Cook, R. M. (2003) Intramolecular dimers: a new design strategy for fluorescence-quenched probes, *Chemistry 9*, 3466–3471.
22. Blum, G., Mullins, S. R., Keren, K., Fonovic, M., Jedeszko, C., Rice, M. J., Sloane, B. F., and Bogyo, M. (2005) Dynamic imaging of protease activity with fluorescently quenched activity-based probes, *Nat. Chem. Biol. 1*, 203–209.
23. Kenworthy, A. K. (2001) Imaging protein-protein interactions using fluorescence resonance energy transfer microscopy, *Methods 24*, 289–296.
24. Adams, S. R., and Tsien, R. Y. (1993) Controlling cell chemistry with caged compounds, *Annu. Rev. Physiol. 55*, 755–784.
25. Karpen, J. W., Zimmerman, A. L., Stryer, L., and Baylor, D. A. (1988) Gating kinetics of the cyclic-GMP-activated channel of retinal rods: flash photolysis and voltage-jump studies, *Proc. Natl. Acad. Sci. U.S.A. 85*, 1287–1291.
26. McCray, J. A., Fidler-Lim, N., Ellis-Davies, G. C., and Kaplan, J. H. (1992) Rate of release of Ca^{2+} following laser photolysis of the DM-nitrophen-Ca^{2+} complex, *Biochemistry 31*, 8856–8861.
27. Bannwarth, M., Correa, I. R., Sztretye, M., Pouvreau, S., Fellay, C., Aebischer, A., Royer, L., Rois, E., and Johnsson, K. (2009) Indo-1 derivatives for local calcium sensing, *ACS Chem. Biol. 4*, 179–190.
28. Misra, A., Kumar, P., and Gupta, K. C. (2007) Synthesis of hairpin probe using deoxyguanosine as a quencher: Fluorescence and hybridization studies, *Anal. Biochem. 364*, 86–88.
29. Tomat, E., Nolan, E. M., Jaworski, J., and Lippard, S. J. (2008) Organelle-specific zinc detection using zinpyr-labeled fusion proteins in live cells, *J. Am. Chem. Soc. 130*, 15776–15777.
30. Maurel, D., Comps-Agrar, L., Brock, C., Rives, M. L., Bourrier, E., Ayoub, M. A., Bazin, H., Tinel, N., Durroux, T., Prezeau, L., Trinquet, E., and Pin, J. P. (2008) Cell-surface protein-protein interaction analysis with time-resolved FRET and snap-tag technologies: application to GPCR oligomerization, *Nat. Methods 5*, 561–567.
31. Keppler, A., Arrivoli, C., Sironi, L., and Ellenberg, J. (2006) Fluorophores for live cell imaging of AGT fusion proteins across the visible spectrum, *Biotechniques* 41, 167−170, 172, 174−175.
32. McNeil, P. L. (2001) Direct introduction of molecules into cells, *Curr. Protoc. Cell Biol. Chapter 20*, Unit 20.1.
33. Yumura, S., Matsuzaki, R., and Kitanishi-Yumura, T. (1995) Introduction of macromolecules into living Dictyostelium cells by electroporation, *Cell Struct. Funct. 20*, 185–190.
34. McNeil, P. L., and Warder, E. (1987) Glass beads load macromolecules into living cells, *J. Cell Sci. 88*, (Pt 5), 669–678.
35. Burack, W. R., and Shaw, A. S. (2005) Live cell imaging of ERK and MEK: simple binding equilibrium explains the regulated nucleocytoplasmic distribution of ERK, *J. Biol. Chem. 280*, 3832–3837.
36. Gautier, A., Juillerat, A., Heinis, C., Correa, I. R., Jr., Kindermann, M., Beaufils, F., and Johnsson, K. (2008) An engineered protein tag for multiprotein labeling in living cells, *Chem. Biol. 15*, 128–136.
37. Kenworthy, A. K., Nichols, B. J., Remmert, C. L., Hendrix, G. M., Kumar, M., Zimmerberg, J., and Lippincott-Schwartz, J. (2004) Dynamics of putative raft-associated proteins at the cell surface, *J. Cell Biol. 165*, 735–746.
38. Pucadyil, T. J., Kalipatnapu, S., Harikumar, K. G., Rangaraj, N., Karnik, S. S., and Chattopadhyay, A. (2004) G-Protein-dependent cell surface dynamics of the human serotonin 1A receptor tagged to yellow fluorescent protein, *Biochemistry 43*, 15852–15862.
39. Schmidt, K., and Nichols, B. J. (2004) A barrier to lateral diffusion in the cleavage furrow of dividing mammalian cells, *Curr. Biol. 14*, 1002–1006.
40. Gronemeyer, T., Chidley, C., Juillerat, A., Heinis, C., and Johnsson, K. (2006) Directed evolution of O^6-alkylguanine-DNA alkyltransferase for applications in protein labeling, *Protein Eng., Des. Sel. 19*, 309–316.
41. Gautier, A., Nakata, E., Lukinavicius, G., Tan, K. T., and Johnsson, K. (2009) Selective cross-linking of interacting proteins using self-labeling tags, *J. Am. Chem. Soc. 131*, 17954–17962.
42. Soumpasis, D. M. (1983) Theoretical analysis of fluorescence photobleaching recovery experiments, *Biophys. J. 41*, 95–97.
43. Axelrod, D., Koppel, D. E., Schlessinger, J., Elson, E., and Webb, W. W. (1976) Mobility measurement by analysis of fluorescence photobleaching recovery kinetics, *Biophys. J. 16*, 1055–1069.